



# Lupeol against high-glucose-induced apoptosis via enhancing the anti-oxidative stress in rabbit nucleus pulposus cells

Ming-Bo Guo<sup>1</sup> · De-Chun Wang<sup>1</sup> · Hai-Fei Liu<sup>1</sup> · Long-Wei Chen<sup>1</sup> · Jian-Wei Wei<sup>1</sup> · Yong Lin<sup>1</sup> · Hui Xue<sup>1</sup>

Received: 25 October 2017 / Revised: 19 May 2018 / Accepted: 25 June 2018 / Published online: 14 July 2018  
© Springer-Verlag GmbH Germany, part of Springer Nature 2018

## Abstract

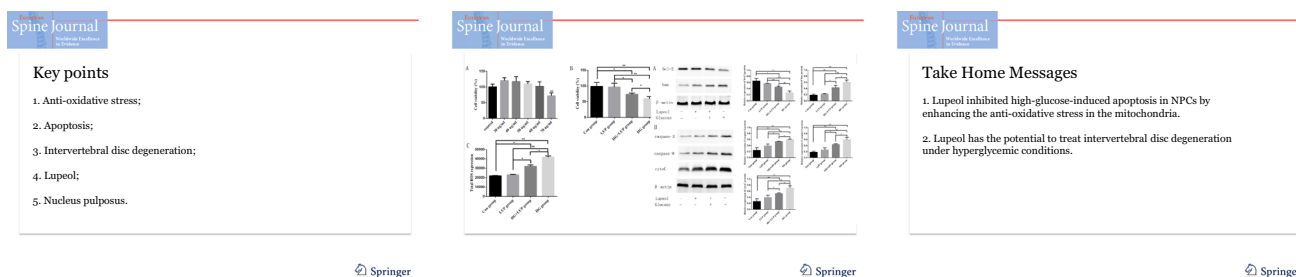
**Purpose** This study aimed to investigate the potential mechanism and value of lupeol in inhibiting high-glucose-induced apoptosis in rabbit nucleus pulposus cells (NPCs).

**Methods** NPCs were divided into four groups: control (CON), high glucose (HG), LUP, and HG + LUP. Viability, reactive oxygen species (ROS) levels, and apoptosis were examined in NPCs. The protein expression levels of Bax, Bcl-2, cytochrome C, and caspase 9/3 were measured using reverse transcription–polymerase chain reaction and Western blot assay.

**Results** The apoptotic rate and total ROS level of the HG group significantly increased compared with the CON group ( $P < 0.01$ ). The total ROS level in the HG + LUP group significantly decreased compared with the HG group ( $P < 0.05$ ). The mRNA expression of Bcl-2 was significantly upregulated, whereas the expression of Bax, cytochrome C, and caspase 9/3 was downregulated in the HG + LUP group compared with those in the HG group ( $P < 0.05$ ). The Western blot assay showed that the expression of Bcl-2 was upregulated, but the expression of Bax, cytochrome C, and caspase 9/3 was significantly downregulated in the HG + LUP group compared with the HG group ( $P < 0.05$ ).

**Conclusions** Lupeol inhibited high-glucose-induced apoptosis in NPCs by enhancing the anti-oxidative stress in the mitochondria. This study suggested lupeol as a potential therapeutic drug for treating intervertebral disc degeneration under hyperglycaemic conditions.

**Graphical abstract** These slides can be retrieved under Electronic Supplementary Material.



**Keywords** Anti-oxidative stress · Apoptosis · Intervertebral disc degeneration · Lupeol · Nucleus pulposus

Ming-Bo Guo and Hai-Fei Liu have contributed equally to this work and should be considered co-first authors.

**Electronic supplementary material** The online version of this article (<https://doi.org/10.1007/s00586-018-5687-9>) contains supplementary material, which is available to authorized users.

✉ De-Chun Wang  
dechun-w@163.com

Extended author information available on the last page of the article

## Introduction

Intervertebral disc degeneration (IDD)-induced secondary spinal instability and spinal stenosis are the main causes of low back pain. The reduction in the number and functions of nucleus pulposus cells (NPCs) is the main cause of IDD. The structure and composition of extracellular matrix begin to change with the reduction in NPCs, accompanied

by the synthetic and catabolic imbalance of extracellular matrix. Meanwhile, the changes in collagen fibre compositions reduce their compressive capacity. Hence, the combined actions of these two contribute to the weakening or loss of mechanical functions of intervertebral discs [1]. The degeneration mechanism of intervertebral disc is not clear yet. Presently, it has been found that the occurrence and development of IDD may be related to genetic susceptibility, senescence, mechanical load, nutritional supply disorder, oxidative stress, diabetes, or other factors [2–4]. Investigating the relationships between these factors and IDD is important for preventing and treating IDD [5, 6].

The pathogenesis of diabetes mellitus-related chronic complications is extremely complex. Some studies have shown that hyperglycaemia is one of the factors inducing apoptosis of intervertebral disc cells [7]. Kong et al. [8] reported that the proliferation of NPCs was significantly inhibited in a high-glucose environment; however, no significant changes were found in a low-glucose environment. The study further demonstrated that excessive production of reactive oxygen species (ROS) was one of the main factors causing the apoptosis of NPCs in hyperglycaemia. Further, hyperglycaemia can induce the production of many advanced glycolic end products, promoting the formation of oxygen free radicals and resulting in the apoptosis of mitochondria through oxidative stress damage [9, 10]. ROS is a class of free radicals related to the oxidative stress, mainly including the superoxide anion ( $O^-$ ), hydroxyl radical ( $-OH$ ),  $H_2O_2$ , and  $NO$ , which can be produced by the mitochondria and catalase in human cells or induced by certain special physicochemical environment [11, 12]. Under normal circumstances, the production and clearance system of reactive oxygen in vivo is in a dynamic equilibrium state [13]. Increased reactive oxygen or decreased clearance ability of reactive oxygen causes oxidative stress [14]. The oxidative stress state can cause DNA oxidative damage and protein expression abnormalities, as well as secondary damages to the body [15]. Therefore, the oxidative stress is not only related to the occurrence and development of many diseases but also closely related to apoptosis.

Lupeol is a triterpenoid compound widely distributed in fruits, vegetables, or Chinese herbal medicines. A large number of animal experiments have demonstrated the anti-oxidative, anti-inflammatory, antibacterial, anti-malarial, anti-apoptosis, anti-malignant tumour proliferation, and anti-neovascularization effects of lupeol [16–18]. Studies have shown that food-derived antioxidants can inhibit the production of ROS, maintain the redox balance, and exert cytoprotective effects to reduce mitochondrial-mediated cell death [18].

The present study hypothesized that lupeol possibly affected the production of ROS and inhibited the apoptosis

of NPCs in a high-glucose environment by antagonizing the oxidative stress.

## Materials and methods

### Isolation and in vitro culture of NPCs

Rabbits were anesthetized with an intraperitoneal injection of 10% chloral hydrate solution (10 mL/kg) and killed by injecting 20 mL of air into the ear vein. The lower thoracic spine and whole lumbar spine were harvested using the aseptic technique. The gel-like NPCs were then scraped using a sterile curette and digested with 0.25% trypsin–EDTA (Sigma-Aldrich, MO, USA) for 30 min at 37 °C on a shaker. The digestion mixture was centrifuged at 1000 rpm for 5 min, and the supernatant was discarded. The tissue pellet was further digested in 0.2% (w/v) collagenase type II (Sigma-Aldrich, MO, USA) at 37 °C for 4 h before filtered through an 80- $\mu$ m sterile nylon mesh filter. The mixture was centrifuged at 1500 rpm for 5 min, and the cell pellets were resuspended in HAM/F-12 + 10% fetal bovine serum (FBS) culture medium. The cell concentration was adjusted to  $(3-5) \times 10^8$ /mL and then seeded into 25-cm<sup>2</sup> cell culture flasks with Dulbecco's modified Eagle's medium (DMEM)/F-12 culture medium (HyClone Company, UT, USA) containing 10% FBS (Biological Industries Company, Israel), penicillin (100 IU/ml), and streptomycin (100 mg/ml) in a humid 5%  $CO_2$  incubator. The culture medium was changed twice a week.

### Identification of NPCs

When the cells converged about 80%, the coverslip was washed with phosphate-buffered saline (PBS) solution, fixed in 4% paraformaldehyde solution, and stained with haematoxylin solution and 1% toluidine blue. Haematoxylin–eosin staining and toluidine blue staining were used to observe cellular morphology under an inverted microscope (Olympus, Japan). The type II collagen was detected with immunohistochemical staining and immunofluorescence detection following standard protocols. The sections were mounted and photographed under an inverted microscope (Olympus, Japan). The immunofluorescence-stained NPCs were observed and photographed under a fluorescence microscope.

### Cytotoxicity assay

Lupeol-containing (L5632, Sigma, Germany) medium was divided into five groups according to different concentration gradients (30, 40, 50, 60, and 70  $\mu$ g/mL) [19]. The cells (density  $1.0 \times 10^5$ /mL) were inoculated into 96-well plates (with 8 wells for each group and 100  $\mu$ L in each

well). The cells of all five groups were cultured in a CO<sub>2</sub> incubator for 24 h. Then, 10 µL of cell counting kit 8 (CCK-8) solution was added into each well for another 2-h incubation in the dark. The optical density (OD) value of each well was detected at 450 nm using a multifunctional orifice plate to determine the cell vitality of each group.

## Experimental design

The third-generation NPCs were randomly divided as follows: (1) CON group: cultured in normal culture medium; (2) HG group: cultured in 100 mM glucose-containing medium; (3) LUP group: cultured in a medium containing an appropriate concentration of lupeol; and (4) HG + LUP group: cultured in a medium containing lupeol and 100 mM glucose. The cell vitality, ROS level, apoptosis rate, and expression of caspase 9/3, Bax, Bcl-2, and cytochrome C proteins and genes of the groups were detected under the same experimental conditions.

## Detection of cell proliferation activity

The cells (density  $1.0 \times 10^5$ /mL) were inoculated into 96-well plates (8 wells for each group and 100 µL in each well) in a CO<sub>2</sub> incubator. When the cells converged 80%, different media were replaced according to the experimental design. The OD value of each well was detected at 450 nm using a spectrophotometer.

## Detection of total intracellular ROS

2', 7'-Dichlorofluorescein diacetate (DCFH-DA) was diluted with serum-free DMEM/F-12 medium in the ratio 1:1000 to reach the final concentration of 10 µM. After a 6-h intervention with different media, the cells were rinsed with PBS (37 °C) two times and digested with trypsin–EDTA for 30–40 s. DMEM/F-12 medium (containing 10% FBS) was added to terminate digestion. The cell suspension was centrifuged (1000 rpm × 5 min), and the supernatant was discarded. The collected cells were resuspended in diluted DCFH-DA (serum-free) and incubated in a CO<sub>2</sub> incubator (37 °C and 5% CO<sub>2</sub>) for 20 min. The cell suspension was centrifuged (1000 rpm × 5 min), and the supernatant was discarded. DMEM/F-12 culture medium was added to resuspend the cells, and the cell count plate was used to calculate the cell concentration. After adjusted the cell density to  $1.0 \times 10^5$ /mL, the cells were inoculated into black 96-well microtiter plates (5 wells for each group and 100 µL in each well) to detect the fluorescence intensity of each group.

## Detection of apoptotic rate

After 6-h intervention with different media, the culture medium in each group was discarded, and the cells were cultured in serum-free DMEM/F-12 for 12 h to terminate the cell proliferation. The digested cells were collected, centrifuged at room temperature at 1000 rpm for 5 min, resuspended in pre-cooled PBS at 4 °C, and centrifuged at 1000 rpm for 5 min. The supernatant was then discarded, and 300 µL of 1× binding buffer was added to suspend the cells. After mixing with 5 µL of Annexin V–fluorescein isothiocyanate (Annexin V), the cells were incubated (serum-free) in the dark at room temperature for 15 min. Then, 5 µL of propidium iodide (PI) was added for 5 min before testing, and 200 µL of 1× binding buffer was also supplemented. In the early apoptotic phase, the membrane of NPCs has phosphatidylserine (PS) eversion phenomenon. Annexin V has the characteristic of specifically binding to PS, while PI is membrane impermeant and generally excluded from NPCs with intact membrane. In the late apoptotic phase, the integrity of NPCs membrane was destroyed, leading to the entrance of PI which could combine with nucleic acids and exhibit positive fluorescence expression. The apoptotic rate was measured using flow cytometry technique [20].

## mRNA expression analysis using reverse transcription–polymerase chain reaction

The cells in each group were incubated for 6 h with different treatments (presence of serum). The total RNA was extracted with TRIzol reagent (Invitrogen, CA, USA) according to the manufacturer's protocol. The total RNA was reverse-transcribed using M-MLV reverse transcriptase (Fermentas China Co, Ltd, Shanghai, China). Real-time polymerase chain reaction (PCR) was performed using the SYBR Green PCR Master Mix (Applied Biosystems, CA, USA) and GeneAmp 5700 Sequence Detection System to detect the mRNA expression of caspase 9/3, Bax, Bcl-2, and cytochrome C.

## Western blot assay

The cells in each group were lysed in extraction buffer with ultrasound on ice, centrifuged, and dialyzed. The extraction buffer was composed of 50 mM Tris HCl (pH 7.4), 150 mM NaCl, 1 mM EDTA, 1% NP-40, 0.5% sodium deoxycholate, 0.1% SDS, 1 mM phenylmethylsulfonyl fluoride, and proteinase inhibitors (1 mg/mL aprotinin, 1 mg/mL pepstatin, and 1 mg/mL leupeptin). The protein concentration of the supernatant was determined. The supernatant samples in the sample buffer were loaded and separated by sodium dodecyl sulphate–polyacrylamide gel electrophoresis, transferred on to polyvinylidene

fluoride membranes, and blocked with 4% nonfat milk at 4 °C overnight. The polyvinylidene fluoride membranes were incubated with rabbit polyclonal caspase 9 p10 antibody (Bioss Inc, Boston, MA, USA, 1:1000), rabbit polyclonal active caspase 3 (Abcam, Cambridge, MA, USA, 1:1000), rabbit polyclonal Bax antibody (Bioss Inc, Boston, MA, USA, 1:1000), rabbit polyclonal Bcl-2 antibody (Bioss Inc, Boston, MA, USA, 1:1000), and rabbit polyclonal cytochrome C antibody (Bioss Inc, Boston, MA, USA, 1:1000) for 24 h. The blots were also probed with an anti- $\beta$ -actin monoclonal antibody (Sigma, St Louis, MO, USA, 1:10,000) as a loading control. The membranes were immersed in PBS with secondary antibodies for 1 h. Cross-reactivity was visualized using enhanced chemiluminescence Western blotting detection reagents (Amersham Pharmacia Biotech, Buckinghamshire, UK) and analysed by scanning densitometry using the Tanon Image System (Tanon, Shanghai, China). The protein expression of caspase 9/3, Bax, Bcl-2, and cytochrome C was analysed.

Experiments were independently conducted three times. Data were reported as mean  $\pm$  SD. Statistical analysis was performed using two-tailed Student *t* test, and a *P* value < 0.05 was considered statistically significant.

## Results

### Growth characteristics of the NPCs

The primary NPCs were spherical shaped after seeding and began to adhere to the culture surface after 3–4 days with a round shape and larger size (Fig. 1a). After the pseudopod was formed, the cells appeared triangular, polygonal, or short spindle in shape with a larger nucleus or two nuclei sometimes. The karyosome was obvious, and the secretory particles could be seen in the cytoplasm. One week later, the pseudopods of the cells connected and formed a network (Fig. 1b). After 15 days of culture, most of the cells were confluent, and matrix-like substances could be seen around the cells (Fig. 1c). About 3 weeks of culture, the primary NPCs fused up to 85% or more (Fig. 1d).

### Different staining assessment of NPCs

The haematoxylin–eosin staining results showed that the NPCs were of polygonal, short spindle, or other irregular shapes (Fig. 2a). After staining with toluidine blue, the accumulated proteoglycans were stained sky blue (Fig. 2b). The nucleus was in the centre of the cell or leaned to one side. The immunofluorescence staining showed the extensive

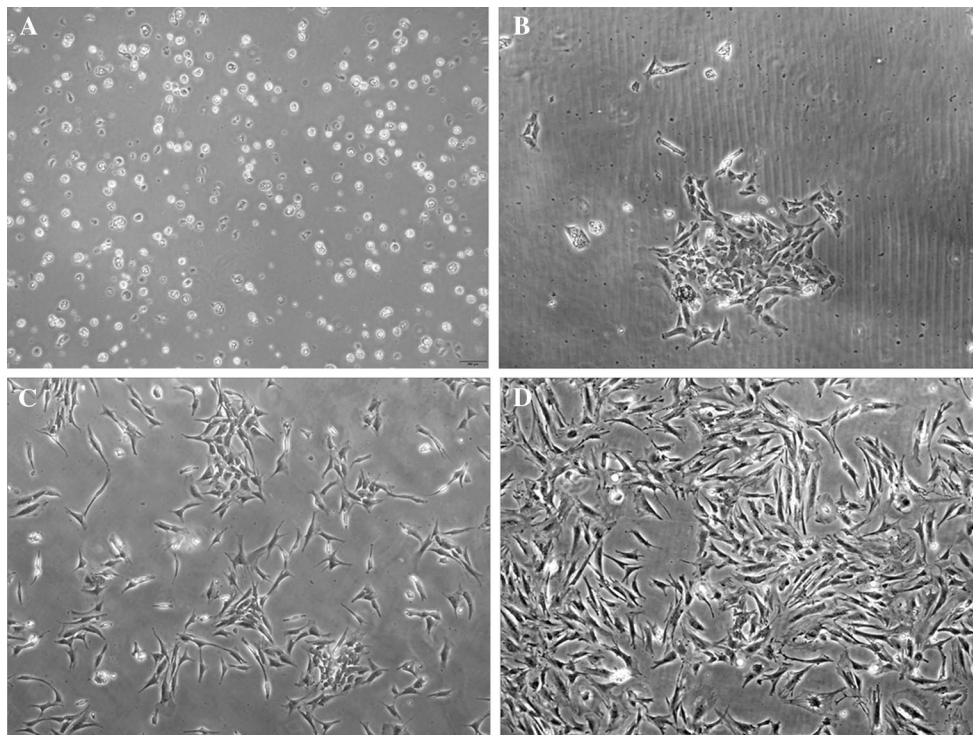


**Fig. 1** Growth characteristics of the NPCs. **a** Cell morphology of primary NPCs after inoculation ( $\times 40$ ). **b** Primary NPCs were cultured for 8 days ( $\times 40$ ). **c** Shape of NPCs after 14 days ( $\times 40$ ). **d** Morphology of NPCs after 21 days of culture ( $\times 40$ )

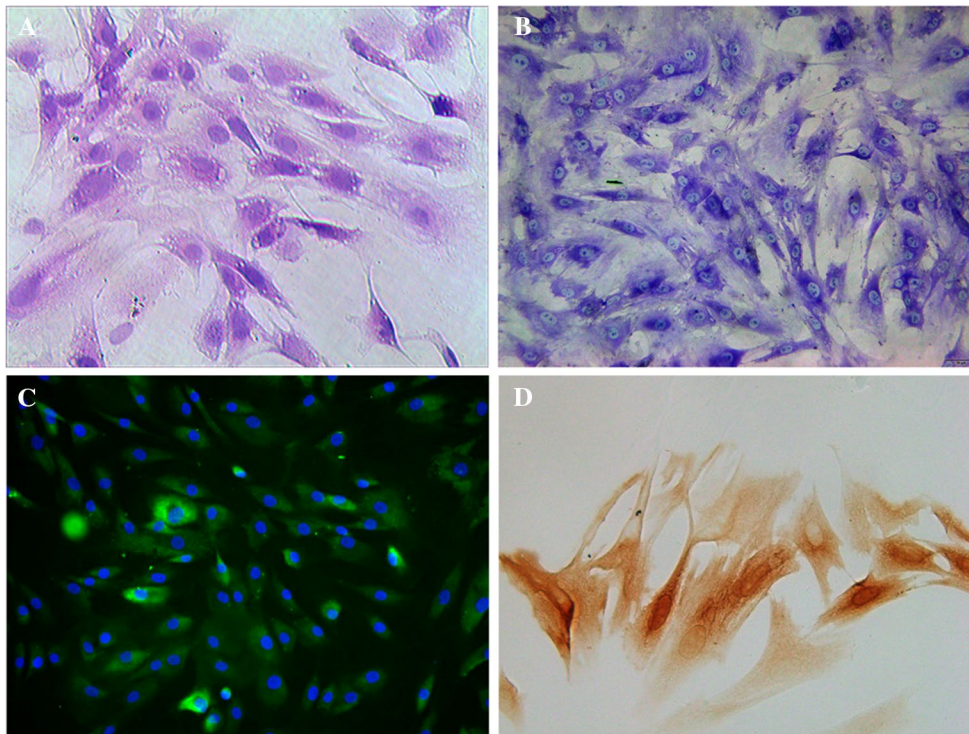


**Fig. 2** Staining assessment of NPCs. **a** Haematoxylin–eosin staining: NPCs were spindle shaped and polygonal, and the nucleus was round or oval ( $\times 200$ ). **b** Toluidine blue staining: NPCs stained strongly positive with toluidine blue ( $\times 200$ ). **c** Immunofluorescence staining: the

cytoplasm showed green fluorescence, and the nucleus showed blue fluorescence ( $\times 200$ ). **d** Immunohistochemical staining: type II collagen in cytoplasm stained yellowish brown ( $\times 400$ )

expression of fluorescence of type II collagen, most of which was located in the cytoplasm. The fluorescence intensity was stronger when closer to the nucleus (Fig. 2c). The nucleus exhibited blue fluorescence. The immunohistochemical staining showed that the type II collagen was stained tan (Fig. 2d).

### Cytotoxicity assay

The results of CCK-8 method (Fig. 3a) showed that when the concentration of lupeol was more than  $60 \mu\text{g/mL}$ , the cell viability was seriously affected ( $P < 0.01$ ) and lupeol had the minimal and similar cytotoxicity when its concentration was below  $60 \mu\text{g/mL}$ . Therefore, the lupeol concentration of  $60 \mu\text{g/mL}$  was used for further experiments.

### Cell proliferation activity

The results of CCK-8 assay showed that the cell proliferation activity in the LUP group was not significantly different from that in the CON group, but the values in the HG group significantly decreased compared with the CON and LUP groups ( $P < 0.01$ ). The HG + LUP group showed increased cell proliferation activity compared with the HG

group ( $P < 0.05$ ). The differences among different groups were statistically significant (Fig. 3b).

### ROS detection

The results of ROS detection in each group are shown in Fig. 3c. The ROS level in the LUP group was not significantly different from that in the CON group. The ROS level in the HG group was significantly higher than that in the CON and HG groups ( $P < 0.01$ ). The ROS values significantly reduced in the HG + LUP group compared with the HG group ( $P < 0.05$ ).

### Cell apoptosis assay

The results of flow cytometry showed that the apoptotic rate of NPCs significantly increased in a high-glucose environment, and the apoptotic rate in the HG + LUP group was significantly different from that in the HG group. Lupeol-treated NPCs exhibited a significantly reduced apoptotic rate. Additionally, no significant difference was found in the apoptotic rates between the LUP and CON groups (Fig. 4).

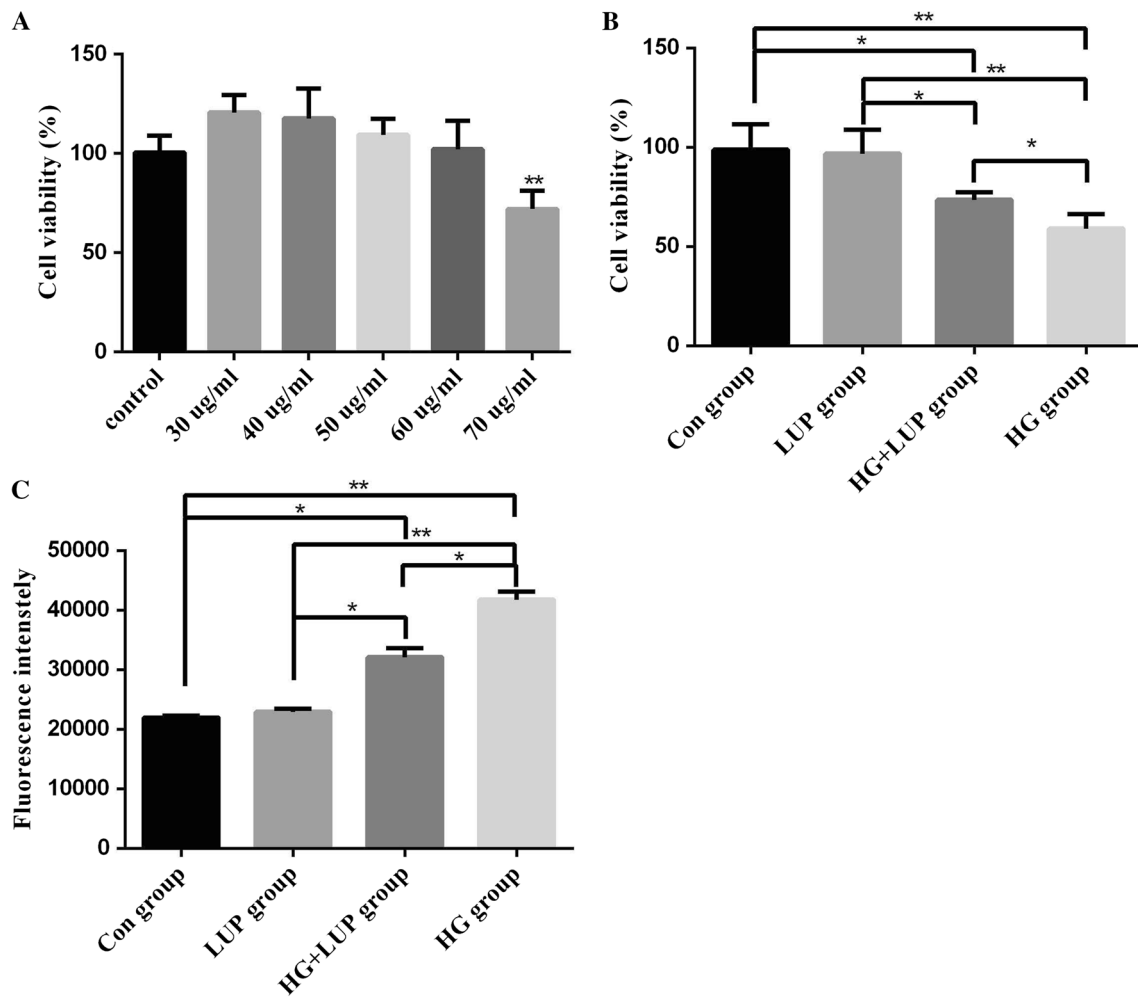


**Fig. 3** Lupeol (LUP) protected NPCs from high-glucose-induced cytotoxicity. **a** Effect of LUP on the activity of NPCs. **b** NP cell viability significantly reduced in the HG group compared with other groups ( $P < 0.01$ ). The activity of NPCs increased significantly in the HG+LUP group than in the HG group ( $P < 0.05$ ). **c** Total ROS

level was detected using fluorophotometry. The generation of ROS significantly increased in the glucose group compared with the control group ( $P < 0.01$ ). The ROS level reduced significantly in the HG+LUP group than in the HG group ( $P < 0.01$ ). (\*\* $P < 0.01$ ; \* $P < 0.05$ )

### mRNA expression assay

The results showed that the expression of caspase 9/3, Bax, and cytochrome C increased significantly, whereas the expression of Bcl-2 was inhibited in the HG group compared with the control group. The expression of Bcl-2 obviously increased, and the expression of caspase 9/3, Bax, and cytochrome significantly declined in the HG+LUP group compared with the HG group (Fig. 5).

### Western blot assay

The expression of Bax, Bcl-2, cytochrome C, and caspase 3/9 was detected by Western blot assay to analyse the protective effect of lupeol on the apoptosis of high-glucose-induced DNPCs. The expression of Bax, cytochrome C,

and caspase 9/3 was significantly upregulated, and the expression of Bcl-2 was downregulated in the HG group compared with the CON group. In HG+LUP group, the expression of Bcl-2 was upregulated and the expression of Bax, cytochrome C, and caspase 9/3 was significantly downregulated in the HG+LUP group compared with the HG group ( $P < 0.05$ ) (Fig. 6).

### Discussion

It has been confirmed that lupeol has a wide range of medicinal values, including strong anti-oxidation, anti-mutation, anti-inflammation, anti-rheumatism, and anti-tumour effects. However, reports on the role of lupeol in the apoptosis of NPCs are rare. The present study found that the apoptotic

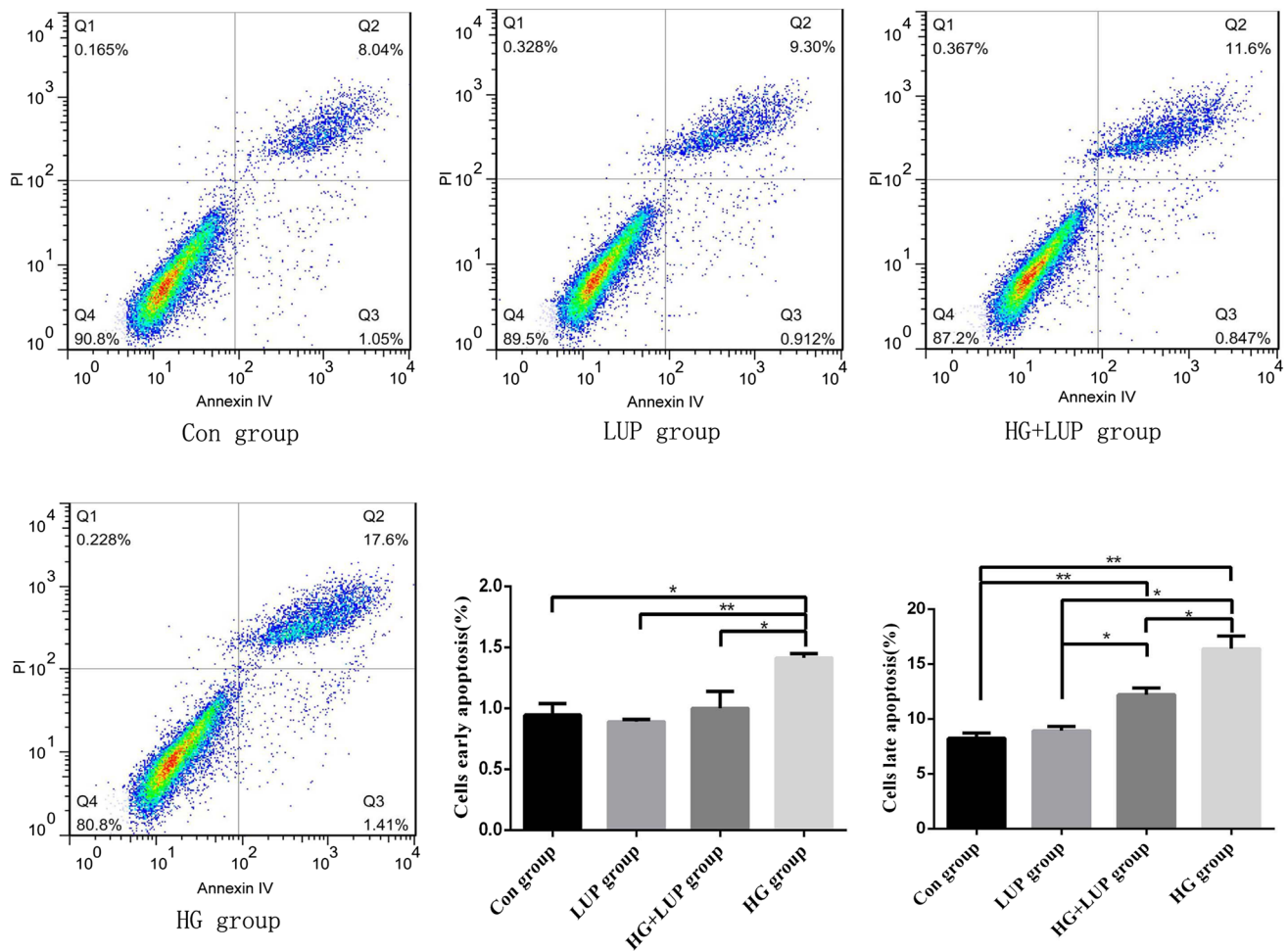


**Fig. 4** Apoptosis was determined by flow cytometry. Early apoptosis (Q3) was demonstrated. Apoptosis significantly increased in the glucose group ( $*P < 0.05$ , compared with the control group). However, apoptosis significantly reduced in the HG+LUP group compared

with the HG group ( $*P < 0.05$ ). In late apoptosis (Q2), the apoptosis rate was remarkably higher in the HG group than in the CON group ( $**P < 0.01$ ). Obviously, the apoptosis rate in the HG+LUP group was lower than that in the HG group ( $*P < 0.05$ )

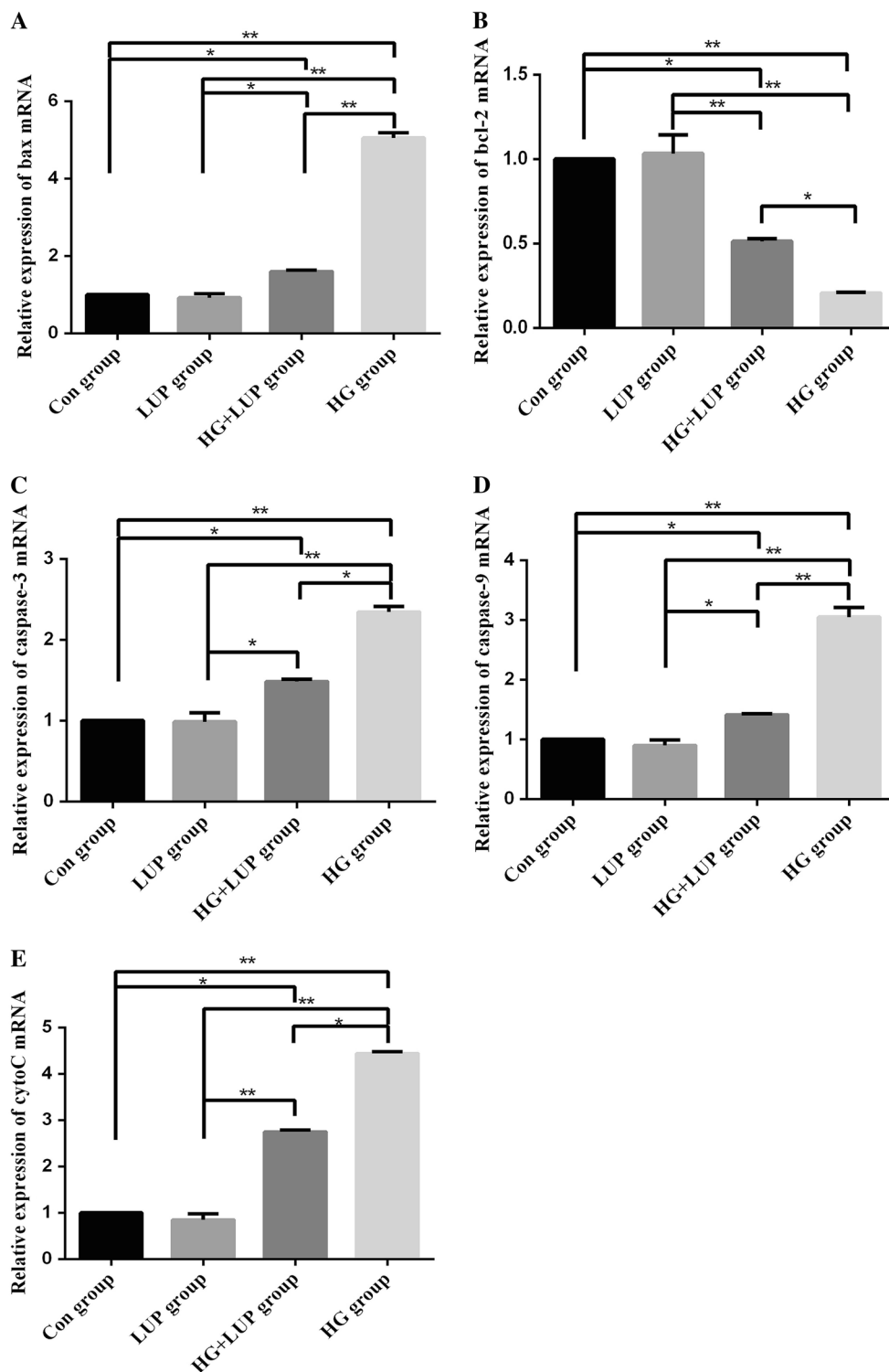
rate of NPCs was significantly higher in the HG group compared with the CON group. Additionally, the apoptosis of NPCs was inhibited in the HG+LUP group compared with the HG group. Therefore, it was suggested that lupeol might inhibit the apoptosis of NPCs in high-glucose environment.

This study explored in details the quantitative alternations of ROS levels and apoptosis-related factors in NPCs under hyperglycaemic conditions with or without lupeol. The results might contribute to a better understanding of the effects of lupeol on increased oxidative stress and apoptosis in a hyperglycaemic environment in NPCs. A previous study showed that the apoptosis rate of NPCs increased in rats with diabetes, so did the subsequent occurrence rate of IDD [21]. In the present study, the HG group exhibited significantly decreased proliferation activity, increased ROS levels, and higher apoptosis rate of NPCs in the early and late stages compared with the CON group. Therefore, it was concluded that hyperglycaemia could significantly inhibit the growth

of NPCs and lead to IDD [22]. The results of the present study were consistent with the findings of previous studies.

Oxidative stress refers to the serious imbalance between the production of free radicals and anti-oxidation defence when the body is exposed to harmful stimuli, resulting in in vivo or intracellular accumulation of ROS, followed by cytotoxicity and tissue injury. Under physiological conditions, free radicals are the necessary materials for cell signalling conduction, but their high reactivity, instability, and roles of mediating cell ageing also cause damage to tissues [23, 24]. It has been found that oxidative stress can lead to the activation of apoptotic signalling pathways, including the activation of caspase 9/3 [25]. An abnormal increase in ROS level can adversely affect cell biochemical events, including DNA damage, lipid oxidation, cell cycle arrest, or mitochondrion-mediated cell death [26, 27]. The current study revealed that the expression of caspase 9/3 in NPCs significantly enhanced under high-glucose conditions, and

**Fig. 5** The mRNA expression of cytochrome C, caspase 9/3, and Bax significantly increased, but the expression of Bcl-2 significantly reduced in the HG group compared with other groups. The HG+LUP group showed significantly decreased mRNA expression of cytochrome C, caspase 9/3, and Bax, but remarkably increased expression of Bcl-2, compared with the HG group (\*\* $P < 0.01$ ; \* $P < 0.05$ )



the apoptotic rate of NPCs in the HG group also increased. The mRNA and protein expression of caspase 9/3 in high-glucose-cultured NPCs was significantly downregulated after the treatment with lupeol, indicating that the oxidative stress injury was inhibited and the cell viability was significantly enhanced. Therefore, it was concluded that lupeol

may conduct some roles by alternating the expression of genes involved in antioxidant protection.

Increased cell apoptosis is an important risk factor for IDD [28]. The present study found significantly increased apoptosis of NPCs in the HG group than in the CON group. Additionally, the HG + LUP group exhibited dramatically



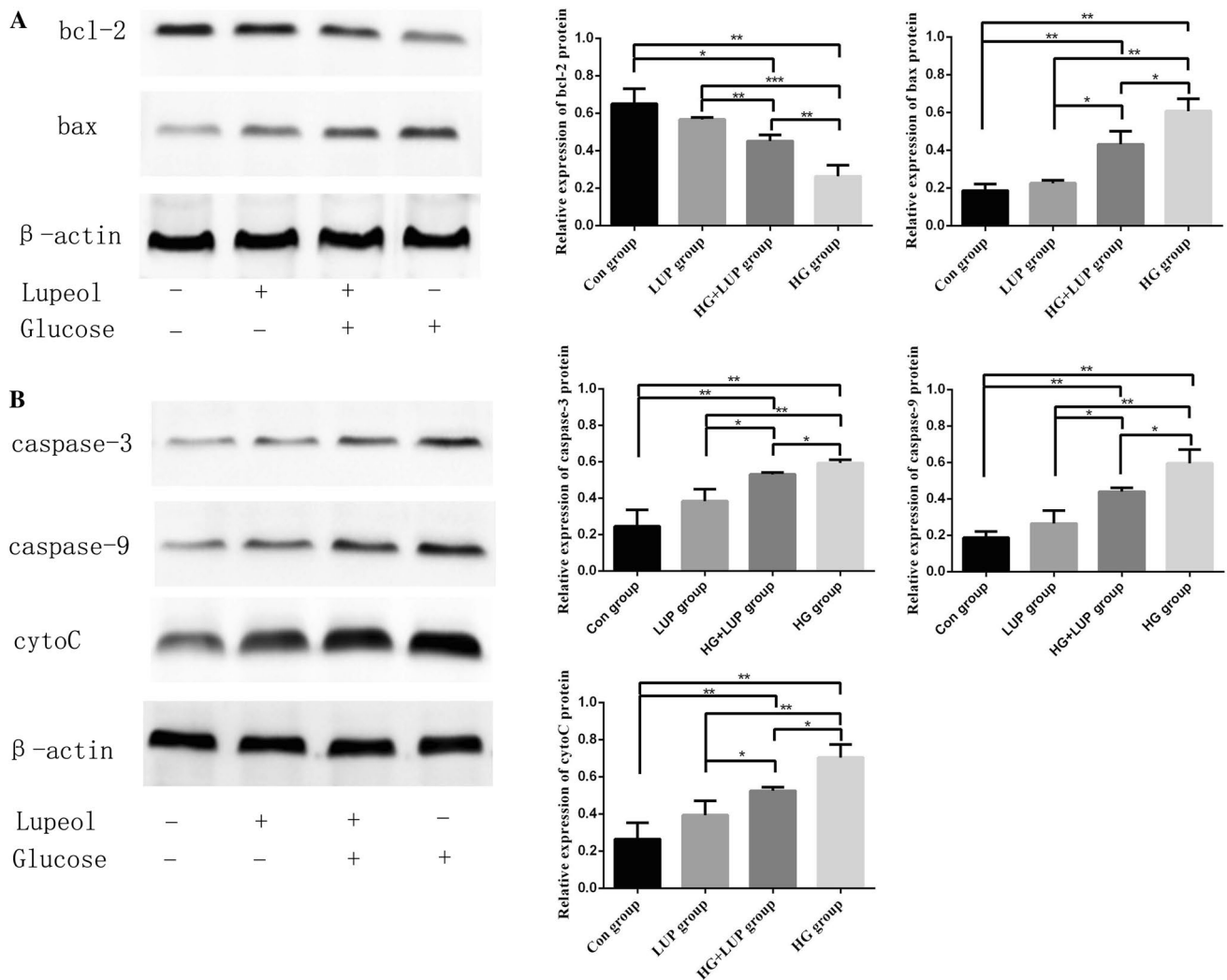


**Fig. 6** Western blot assay for Bcl-2, Bax, caspase 9/3, and cytochrome C. In the HG group, the grey scales for Bax, cytochrome C, and caspase 9/3 were significantly higher than other groups. However, the grey scale for Bcl-2 was remarkably lower in the HG group than in other groups. In the HG+LUP group, the grey scales of Bax,

cytochrome C, and caspase 9/3 were significantly descended, but the value of Bcl-2 was significantly increased, when compared with those in the HG group. No significant differences were found in the expression of all proteins between the LUP and CON groups (\* $P < 0.05$ ; \*\* $P < 0.01$ )

reduced apoptosis of NPCs compared with the HG group. The intrinsic mechanism underlying the effects of lupeol on apoptosis of NPCs in hyperglycaemic environment was further investigated in the present study.

Bcl-2 family proteins are important regulators of apoptosis involved in regulating the changes in the mitochondrial membrane permeability. Bcl-2 family proteins are divided into anti-apoptotic proteins (such as Bcl-2) and pro-apoptotic proteins (such as Bax). When the mitochondrial membrane depolarizes, the membrane permeability changes, and the Bcl-2/Bax ratio also changes. The Bcl-2/Bax ratio determines the fate of cells [29]. Apoptotic protein Bcl-2 can inhibit the occurrence of apoptosis, but Bax promotes the pathogenesis of apoptosis. Bcl-2 is located mainly in the mitochondrial outer membrane and can block the changes

in membrane permeability. However, Bax is transported from the cytoplasm to the mitochondria and can promote the mitochondrial membrane permeability and release of cytochrome C [30]. Downregulating Bcl-2 while upregulating Bax can cause changes in mitochondrial permeability, collapse of mitochondrial membrane potential, and sustained oxidative stress, thus resulting in the significant increase in ROS level and further damages to the mitochondria, eventually leading to the release of cytochrome C and expression of caspase 9/3, and triggering apoptosis. The Bcl-2/Bax ratio and the expression of caspase 3 have been demonstrated to be important indicators for evaluating cell apoptosis [31]. The reverse transcription–PCR results of this study revealed the increased expression of Bax gene and decreased expression of Bcl-2 gene in the HG group than in the HG+LUP

group. The mRNA expression of cytochrome C and caspases 9/3 also significantly decreased in the HG group. The results of mRNA expression were confirmed by the quantitative protein analysis.

One of the important markers of mitochondrial dysfunction is the excessive production of ROS, and it can affect the death process of many cells [32]. In a high-glucose environment, NPCs produce excessive ROS and experience oxidative stress injury, leading to the depolarization of mitochondrial membrane, change in the Bcl-2/Bax ratio, and overexpression of cytochrome C and caspase 9/3. The following activation of mitochondrion-mediated apoptosis pathway eventually results in apoptosis. In this study, the increased expression of Bcl-2 and decreased expression of Bax in the NPCs were observed in the HG + LUP group compared with the HG group, inhibiting oxidative stress injury and maintaining cell viability. In addition, the lupeol significantly inhibited the expression of cytochrome C and caspases 9/3 in NPCs cultured under hyperglycaemic conditions, thereby preventing DNA damage and cell death.

In addition to the intrinsic effects on the apoptosis and oxidative stress in NPCs, high glucose was demonstrated to create a hyperosmotic environment in the culture media, which could diversely affect matrix gene expression, cell proliferation, and biosynthesis activity of NPCs. Wuertz et al. [33] demonstrated that disc cells responded strongly to changes in the osmotic environment by altering mRNA expression. Under increasing osmolarity, human cells increased mRNA expression of aggrecan and collagen II in both nucleus and annulus cells. Collagen I expression was inhibited at high osmolality. Neidlinger-Wilke C et al. [34] also observed increased mRNA expression of aggrecan and diminished mRNA expression of MMP-3 with the increase in osmolality in culture media. Ishihara et al. [35] reported that proteoglycan synthesis rate in bovine NP tissue was upregulated by 200% when the medium osmolarity was raised from 280 to 430 mOsm/kg. However, Chen et al. [36] demonstrated that gene expression of small proteoglycans was downregulated in hypo-osmotic (255 mOsm/kg) or hyperosmotic (450 mOsm/kg) conditions compared to iso-osmotic conditions (293 mOsm/kg). In the studies by Mavrogenatou et al. [37, 38], hyperosmotic stress provoked DNA damage to NPCs which subsequently triggers an enhanced DNA repair response. NPCs' proliferation declined in a dose-dependent manner after medium osmolality was increased. The inhibition of cell proliferation was through the activation of p38 MAPK and p53.

According to these studies, intervertebral disc cells exhibited different alternations in mRNA expression, DNA response, cell proliferation, and matrix protein expression in hyperosmotic environment. Despite of the diverse effects of high-glucose-induced hyperosmolarity on disc cells, the alternation of osmolarity is always accompanied

with high glucose either in the cell research in vitro or in the animal and human study in vivo. In patients with diabetes, the osmotic pressure of blood and extracellular matrix is higher than that of healthy people. In our study, the action environment of lupeol was not with normal osmotic pressure, but with hyperosmotic pressure induced by high glucose, which was consistent with the inner environment of diabetics. The in situ NP osmotic pressure cycles between approximate 450 and 550 mOsm throughout the day [39]. In our future study, the effects of different glucose additions on the final osmolality would be further evaluated and investigated.

This study had certain limitations. Lupeol inhibited high-glucose-induced apoptosis of NPCs, but the study could not determine whether other anti-apoptotic pathways were involved in the process. Further studies are needed to investigate the other effects of lupeol. Moreover, changes in osmotic pressure caused by high glucose may also lead to the expression of apoptotic proteins. The relation between high-glucose-induced hyperosmolarity and oxidative stress, as well as the molecular effects of lupeol on NPCs under hyperosmotic stress, merits deep research. Additionally, rodents (rats and mice) and lagomorphs (e.g. rabbits) maintain a percentage of notochordal cells in their intervertebral discs throughout their lifetime, whereas in human and other animals such as bovine, goat, and sheep, these cells disappear early in lifetime [40, 41]. Further investigations using more appropriate animal models are needed both in vitro and in vivo, before the actual transition.

## Conclusions

The results suggested that lupeol could inhibit ROS-induced cell death in high-glucose environment and maintain the redox balance. Lupeol mitigated the mitochondrion-mediated endogenous apoptotic pathways, promoted the expression of Bcl-2, inhibited the expression of Bax, and prevented the release of cytochrome C into the cytoplasm and activation of caspase 9/3. Lupeol had the potential to inhibit the high-glucose-induced apoptosis in NPCs by enhancing the anti-oxidative stress in the mitochondria, thereby providing new ideas for future treatment of IDD under hyperglycaemia conditions.

**Acknowledgements** This work was supported by the National Natural Science Foundation of China (Grant Nos. 21472104, 81401828) and Qingdao Outstanding Health Professional Development Fund.

## Compliance with ethical standards

**Conflict of interest** The authors declare that they have no conflict of interest.

## References

- Sivan SS, Tsitron E, Wachtel E, Roughley PJ, Sakkee N, van der Ham F, DeGroot J, Roberts S, Maroudas A (2006) Aggrecan turnover in human intervertebral disc as determined by the racemization of aspartic acid. *J Biol Chem* 281:13009–13014. <https://doi.org/10.1074/jbc.M600296200>
- Samartzis D, Karppinen J, Chan D, Luk KD, Cheung KM (2012) The association of lumbar intervertebral disc degeneration on magnetic resonance imaging with body mass index in overweight and obese adults: a population-based study. *Arthritis Rheum* 64:1488–1496. <https://doi.org/10.1002/art.33462>
- Williams FM, Popham M, Sambrook PN, Jones AF, Spector TD, MacGregor AJ (2011) Progression of lumbar disc degeneration over a decade: a heritability study. *Ann Rheum Dis* 70:1203–1207. <https://doi.org/10.1136/ard.2010.146001>
- Potier E, Ito K (2014) Can notochordal cells promote bone marrow stromal cell potential for nucleus pulposus enrichment? A simplified in vitro system. *Tissue Eng Part A* 20:3241–3251. <https://doi.org/10.1089/ten.TEA.2013.0703>
- Battie MC, Videman T, Levalahti E, Gill K, Kaprio J (2008) Genetic and environmental effects on disc degeneration by phenotype and spinal level: a multivariate twin study. *Spine* 33:2801–2808. <https://doi.org/10.1097/BRS.0b013e31818043b7>
- Jiang L, Yuan F, Yin X, Dong J (2014) Responses and adaptations of intervertebral disc cells to microenvironmental stress: a possible central role of autophagy in the adaptive mechanism. *Connect Tissue Res* 55:311–321. <https://doi.org/10.3109/03008207.2014.942419>
- Won HY, Park JB, Park EY, Riew KD (2009) Effect of hyperglycemia on apoptosis of notochordal cells and intervertebral disc degeneration in diabetic rats. *J Neurosurg Spine* 11:741–748. <https://doi.org/10.3171/2009.6.SPINE09198>
- Kong CG, Park JB, Kim MS, Park EY (2014) High glucose accelerates autophagy in adult rat intervertebral disc cells. *Asian Spine J* 8:543–548. <https://doi.org/10.4184/asj.2014.8.5.543>
- Jazini E, Sharan AD, Morse LJ, Dyke JP, Aronowitz EB, Chen LK, Tang SY (2012) Alterations in T2 relaxation magnetic resonance imaging of the ovine intervertebral disc due to nonenzymatic glycation. *Spine* 37:E209–E215. <https://doi.org/10.1097/BRS.0b013e31822ce81f>
- Karim L, Tang SY, Sroga GE, Vashishth D (2013) Differences in non-enzymatic glycation and collagen cross-links between human cortical and cancellous bone. *Osteoporos Int* 24:2441–2447. <https://doi.org/10.1007/s00198-013-2319-4>
- Apel K, Hirt H (2004) Reactive oxygen species: metabolism, oxidative stress, and signal transduction. *Annu Rev Plant Biol* 55:373–399. <https://doi.org/10.1146/annurev.arplant.55.031903.141701>
- Rodriguez R, Redman R (2005) Balancing the generation and elimination of reactive oxygen species. *Proc Natl Acad Sci USA* 102:3175–3176. <https://doi.org/10.1073/pnas.0500367102>
- Yan W, Arai A, Aoki M, Ichijo H, Miura O (2007) ASK1 is activated by arsenic trioxide in leukemic cells through accumulation of reactive oxygen species and may play a negative role in induction of apoptosis. *Biochem Biophys Res Commun* 355:1038–1044. <https://doi.org/10.1016/j.bbrc.2007.02.064>
- Miyamoto H, Doita M, Nishida K, Yamamoto T, Sumi M, Kurosaka M (2006) Effects of cyclic mechanical stress on the production of inflammatory agents by nucleus pulposus and annulus fibrosus derived cells in vitro. *Spine* 31:4–9
- Wang YJ, Shi Q, Lu WW, Cheung KC, Darowish M, Li TF, Dong YF, Zhou CJ, Zhou Q, Hu ZJ, Liu M, Bian Q, Li CG, Luk KD, Leong JC (2006) Cervical intervertebral disc degeneration induced by unbalanced dynamic and static forces: a novel in vivo rat model. *Spine* 31:1532–1538. <https://doi.org/10.1097/01.brs.0000222019.84095.23>
- Siddique HR, Saleem M (2011) Beneficial health effects of lupeol triterpene: a review of preclinical studies. *Life Sci* 88:285–293. <https://doi.org/10.1016/j.lfs.2010.11.020>
- Lima LM, Perazzo FF, Tavares Carvalho JC, Bastos JK (2007) Anti-inflammatory and analgesic activities of the ethanolic extracts from *Zanthoxylum riedelianum* (Rutaceae) leaves and stem bark. *J Pharm Pharmacol* 59:1151–1158. <https://doi.org/10.1211/jpp.59.8.0014>
- Kumari A, Kakkar P (2012) Lupeol prevents acetaminophen-induced in vivo hepatotoxicity by altering the Bax/Bcl-2 and oxidative stress-mediated mitochondrial signaling cascade. *Life Sci* 90:561–570. <https://doi.org/10.1016/j.lfs.2012.01.012>
- Srivastava AK, Mishra S, Ali W, Shukla Y (2016) Protective effects of lupeol against mancozeb-induced genotoxicity in cultured human lymphocytes. *Phytomedicine* 23:714–724. <https://doi.org/10.1016/j.phymed.2016.03.010>
- Evens AM, Prachand S, Shi B, Paniaqua M, Gordon LI, Gartenhaus RB (2004) Imexon-induced apoptosis in multiple myeloma tumor cells is caspase-8 dependent. *Clin Cancer Res* 10:1481–1491
- Anekstein Y, Smorgick Y, Lotan R, Agar G, Shalmon E, Floman Y, Mirovsky Y (2010) Diabetes mellitus as a risk factor for the development of lumbar spinal stenosis. *IMAJ* 12:16–20
- Zhang CX, Wang T, Ma JF, Liu Y, Zhou ZG, Wang DC (2017) Protective effect of CDDO-ethyl amide against high-glucose-induced oxidative injury via the Nrf2/HO-1 pathway. *Spine J* 17:1017–1025. <https://doi.org/10.1016/j.spinee.2017.03.015>
- Yudoh K, Nguyen VT, Nakamura H, Hongo-Masuko K, Kato T, Nishioka K (2005) Potential involvement of oxidative stress in cartilage senescence and development of osteoarthritis: oxidative stress induces chondrocyte telomere instability and downregulation of chondrocyte function. *Arthritis Res Ther* 7:R380–R391. <https://doi.org/10.1186/ar1499>
- Jallali N, Ridha H, Thrasivoulou C, Underwood C, Butler PE, Cowen T (2005) Vulnerability to ROS-induced cell death in ageing articular cartilage: the role of antioxidant enzyme activity. *Osteoarthr Cartil* 13:614–622. <https://doi.org/10.1016/j.joca.2005.02.011>
- Kim KW, Ha KY, Lee JS, Rhyu KW, An HS, Woo YK (2007) The apoptotic effects of oxidative stress and antiapoptotic effects of caspase inhibitors on rat notochordal cells. *Spine* 32:2443–2448. <https://doi.org/10.1097/BRS.0b013e318157395a>
- Kakkar P, Singh BK (2007) Mitochondria: a hub of redox activities and cellular distress control. *Mol Cell Biochem* 305:235–253. <https://doi.org/10.1007/s11010-007-9520-8>
- Singh BK, Tripathi M, Pandey PK, Kakkar P (2010) Nimesulide aggravates redox imbalance and calcium dependent mitochondrial permeability transition leading to dysfunction in vitro. *Toxicology* 275:1–9. <https://doi.org/10.1016/j.tox.2010.05.001>
- Heyde CE, Tschoeke SK, Hellmuth M, Hostmann A, Ertel W, Oberholzer A (2006) Trauma induces apoptosis in human thoracolumbar intervertebral discs. *BMC Clin Pathol* 6:5. <https://doi.org/10.1186/1472-6890-6-5>
- Kumari A, Kakkar P (2012) Lupeol protects against acetaminophen-induced oxidative stress and cell death in rat primary hepatocytes. *Food Chem Toxicol* 50:1781–1789. <https://doi.org/10.1016/j.fct.2012.02.042>
- Pham TN, Marion M, Denizeau F, Jumarie C (2006) Cadmium-induced apoptosis in rat hepatocytes does not necessarily involve caspase-dependent pathways. *Toxicol Vitro* 20:1331–1342. <https://doi.org/10.1016/j.tiv.2006.05.005>
- Prasad S, Kalra N, Shukla Y (2008) Induction of apoptosis by lupeol and mango extract in mouse prostate and LNCaP cells.

- Nutr Cancer 60:120–130. <https://doi.org/10.1080/01635580701613772>
32. Boelsterli UA (2003) Idiosyncratic drug hepatotoxicity revisited: new insights from mechanistic toxicology. *Toxicol Mech Methods* 13:3–20. <https://doi.org/10.1080/15376510309824>
  33. Wuertz K, Urban JP, Klasen J, Ignatius A, Wilke HJ, Claes L, Neidlinger-Wilke C (2007) Influence of extracellular osmolality and mechanical stimulation on gene expression of intervertebral disc cells. *J Orthop Res* 25:1513–1522. <https://doi.org/10.1002/jor.20436>
  34. Neidlinger-Wilke C, Mietsch A, Rinkler C, Wilke HJ, Ignatius A, Urban J (2012) Interactions of environmental conditions and mechanical loads have influence on matrix turnover by nucleus pulposus cells. *J Orthop Res* 30:112–121. <https://doi.org/10.1002/jor.21481>
  35. Ishihara H, Warensjo K, Roberts S, Urban JP (1997) Proteoglycan synthesis in the intervertebral disk nucleus: the role of extracellular osmolality. *Am J Physiol* 272:C1499–C1506. <https://doi.org/10.1152/ajpcell.1997.272.5.C1499>
  36. Chen J, Baer AE, Paik PY, Yan W, Setton LA (2002) Matrix protein gene expression in intervertebral disc cells subjected to altered osmolality. *Biochem Biophys Res Commun* 293:932–938. [https://doi.org/10.1016/S0006-291X\(02\)00314-5](https://doi.org/10.1016/S0006-291X(02)00314-5)
  37. Mavrogenatou E, Kletsas D (2009) High osmolality activates the G1 and G2 cell cycle checkpoints and affects the DNA integrity of nucleus pulposus intervertebral disc cells triggering an enhanced DNA repair response. *DNA Repair* 8:930–943. <https://doi.org/10.1016/j.dnarep.2009.05.005>
  38. Mavrogenatou E, Papadimitriou K, Urban JP, Papadopoulos V, Kletsas D (2015) Deficiency in the alpha1 subunit of Na<sup>+</sup>/K<sup>+</sup>-ATPase enhances the anti-proliferative effect of high osmolality in nucleus pulposus intervertebral disc cells. *J Cell Physiol* 230:3037–3048. <https://doi.org/10.1002/jcp.25040>
  39. Urban JP (2002) The role of the physicochemical environment in determining disc cell behaviour. *Biochem Soc Trans* 30:858–864. <https://doi.org/10.1042/bst0300858>
  40. Hunter CJ, Matyas JR, Duncan NA (2003) The notochordal cell in the nucleus pulposus: a review in the context of tissue engineering. *Tissue Eng* 9:667–677. <https://doi.org/10.1089/107632703768247368>
  41. Hunter CJ, Matyas JR, Duncan NA (2004) Cytomorphology of notochordal and chondrocytic cells from the nucleus pulposus: a species comparison. *J Anat* 205:357–362. <https://doi.org/10.1111/j.0021-8782.2004.00352.x>

## Affiliations

Ming-Bo Guo<sup>1</sup> · De-Chun Wang<sup>1</sup>  · Hai-Fei Liu<sup>1</sup> · Long-Wei Chen<sup>1</sup> · Jian-Wei Wei<sup>1</sup> · Yong Lin<sup>1</sup> · Hui Xue<sup>1</sup>

<sup>1</sup> Qingdao Spine Center, Qingdao Municipal Hospital, Qingdao University, Qingdao 266061, China